

# A Path-Following Guidance Method for Nonholonomic Vehicles with a Large Domain of Attraction for Straight and Curved Paths

Manuel C.R.M. Fernandes and Fernando A.C.C. Fontes.

**Abstract**—Path-following control is an alternative technique to trajectory tracking, with superior performance characteristics when applied to a class of nonholonomic systems, especially relevant in the case of unmanned vehicles. In this work, we study a variant of a well-known guidance logic path-following control and analyze its stability. In particular, we show that the studied method not only maintains the stabilizing properties in a neighborhood of the path, but significantly enlarges the domain of attraction of the control law, both when following a straight or a curved path.

**Index Terms**—Path-Following, Nonholonomic Vehicles, Non-linear Control, Stability Analysis.

## I. INTRODUCTION

Path-following control has been studied in recent years as an alternative formulation to trajectory-tracking, with advantages on the performance of the former, as shown in research on performance limitations for each formulation [1]. While in trajectory-tracking the control law drives the vehicle to follow a time-parameterized reference (i.e., a geometric path with an associated timing law), in path-following the aim is to follow closely just a geometric path in space, without a specific time instant associated with each space location. The speed at which the path is followed can be controlled separately, also without compromising performance.

The theoretical advantage over traditional trajectory-tracking, allied to the importance of guidance laws in unmanned vehicles research has, not surprisingly, fostered an extensive literature on path-following control, examples of which are the recent work [2], the survey [3], and the many references therein.

This work addresses the stability analysis of a path-following guidance logic. The guidance law studied here –termed “L0 Guidance Control” – is a modification of the one presented in [4] and [5], frequently known as “L1 Guidance Control”. Both methods control the heading angle of a nonholonomic vehicle by computing the required centripetal acceleration for the vehicle to join a given path at a determined target reference point ahead on the path, only differing on the tuning parameter that defines the target point: while in the L1 guidance the tuning parameter is the distance from the vehicle to the target point – the  $L_1$  vector magnitude – in the L0 guidance law the tuning parameter

is the distance *along the path* to the target point – the  $L_0$  vector magnitude. The modification of the tuning parameter does not significantly affect the performance, nor the stability guarantees in a neighborhood of the path. However, selecting a fixed  $L_0$  instead of  $L_1$  significantly enlarges the domain of attraction of the control law, with positive consequences on the robustness of the guidance logic and avoiding the necessity of switching controllers when the distance to the path is larger than  $L_1$ .

The “L0 Guidance Control” was first presented in [6], with a proof of stability for straight paths and where it is applied to Airborne Wind Energy Systems. It is given by an explicit formula that can be easily computed from known parameters. It was also used as a basis controller for a Model Predictive Control combined strategy in [7]. The performance of both L0 and L1 controllers is compared for control of tethered aircraft within the context of Airborne Wind Energy Systems in [8].

One of the main contributions in this work is to provide proof of stability of systems following curved paths controlled by the L0 law, completing the work of [6]. It is shown that a nonholonomic system, possibly constrained by a minimum turning radius, can be made to converge to the path from within a large basin of attraction.

This paper is organized as follows. In Section II we define the path-following problem and the type of nonholonomic systems to which this controller is applied to. In Section III, we describe the guidance logic addressed – the L0 guidance controller. In Section IV, we discuss the stability results, providing the proof of stability for both straight and curved paths.

## II. PATH-FOLLOWING

We address the path-following problem for nonholonomic vehicles with car-like constraints, *i.e.* vehicles that cannot turn on themselves and that have bounded curvature trajectories.

The kinematics of such systems can be generally described by the following equations of motion

$$\begin{cases} \dot{x} = V \cos(\psi) \\ \dot{y} = V \sin(\psi) \\ \dot{\psi} = Vc, \end{cases} \quad (1)$$

where  $x$  and  $y$  represent the vehicle’s position cartesian coordinates ( $\mathbf{p} = (x, y)$ ) in a global reference frame. The angle  $\psi$  represents the vehicle’s heading angle, which is the angle between the vehicle’s velocity  $\vec{V} = (\dot{x}, \dot{y})$  and the  $xx$  axis and  $V = \|\vec{V}\|$ . The curvature of the trajectory

This research is supported by FCT/MCTES(PIDDAC), through projects 2022.02320.PTDC-KEFCODE, and 2022.02801.PTDC-UPWIND-ATOL (<https://doi.org/10.54499/2022.02801.PTDC>).

Manuel C.R.M. Fernandes and Fernando A.C.C. Fontes are with SYSTEC-ISR-ARISE and the Department of Electrical and Computer Engineering, Faculty of Engineering, University of Porto, Rua Dr. Roberto Frias, 4200-465 Porto, Portugal. Emails: mcrmf@fe.up.pt, faf@fe.up.pt

TABLE I  
NOMENCLATURE

$c$	vehicle curvature [rad/m]
$d$	cross-track error [m]
$m$	mass [kg]
$x, y$	cartesian coordinates of vehicle position [m]
$\mathbf{p}$	vehicle position [m]
$Q$	closest point on the path to the vehicle position
$R$	reference target point on the path
$R'$	reference target point on the tangent straight path
$R_0$	path curvature radius [m]
$R_{min}$	vehicle minimum curvature radius [m]
$\vec{L}_0$	vector joining points $Q$ and $R$
$\vec{L}_1$	vector joining points $\mathbf{p}$ and $R$
$\vec{L}'_0$	vector joining points $Q$ and $R'$
$\vec{L}'_1$	vector joining points $\mathbf{p}$ and $R'$
$\vec{V}, V$	vehicle velocity vector and magnitude [ $m s^{-1}$ ]
$\eta$	angle between vehicle velocity and vector $\vec{L}_1$ [rad]
$\eta_2$	angle between vehicle velocity and vector $\vec{L}_0$ [rad]
$\eta_1$	angle between vector $\vec{L}_0$ and vector $\vec{L}_1$ [rad]
$\eta'$	angle between vehicle velocity and vector $\vec{L}'_1$ [rad]
$\eta'_2$	angle between vehicle velocity and vector $\vec{L}'_0$ [rad]
$\eta'_1$	angle between vector $\vec{L}'_0$ and vector $\vec{L}'_1$ [rad]
$\gamma$	half the angle of the arc joining $Q$ and $R$ [rad]
$\psi$	vehicle heading angle [rad]

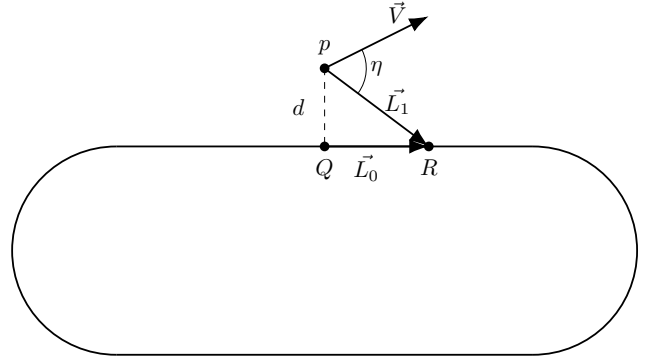


Fig. 1. L0/L1 Guidance Logic variables [6].

is defined by  $c$ , where  $|c|$  is the inverse of the radius of curvature of the trajectory. The vehicle has a minimum turning radius  $R_{min}$ , imposing an input constraint on the curvature  $c \in [-1/R_{min}, 1/R_{min}]$ .

Given a reference trajectory  $t \mapsto (x_{ref}(t), y_{ref}(t)) : [0, T] \rightarrow \mathbb{R}^2$  and the corresponding reference path  $\{(x_r, y_r) \in \mathbb{R}^2 : x_r = x_{ref}(t), y_r = y_{ref}(t), t \in [0, T]\}$ , we can represent the behaviour of the vehicle relative to a reference path instead of the global reference frame, using the relative coordinates  $(d, \eta)$ , where  $d$  is the cross-track error and  $\eta$  is the error on the desired bearing. Considering that the vehicle is off the path in position  $\mathbf{p}$ , that  $Q$  is its closest point on the path, and  $R$  is a reference point ahead on the path (see Fig. 1), then  $d$  is the distance from  $\mathbf{p}$  to  $Q$  and  $\eta$  is the angle between the vehicle's velocity vector and the vector joining  $\mathbf{p}$  to  $R$ . When the variables  $(d, \eta)$  are both equal to 0, the vehicle's adherence to the path is perfect.

### III. GUIDANCE LOGIC

#### A. Heading Angle Control

The L0 guidance logic uses a reference target in the path in order to compute the required centripetal acceleration to follow that reference, depending on the selected parameter  $L_0$ . Firstly, given the coordinates  $\mathbf{p}(x, y)$  of the vehicle's centre of mass, we determine the closest point in the path to the vehicle  $Q$ . We then define our reference target point  $R$  as the point ahead in the path distancing  $L_0$  from point  $Q$ , as is shown for the straight path case in Figure 1. We are now able to define the vector  $\vec{L}_1$ , which is the vector joining the vehicle's current position  $\mathbf{p}$  and the reference target point  $R$ . We then compute the angle  $\eta$  which is the angle between the vehicle velocity vector  $\vec{V}$  and  $\vec{L}_1$ . Finally, it is now possible to compute the required centripetal acceleration for

the vehicle to perform a curved trajectory joining the path in  $R$  using the following equation:

$$a_s = 2 \frac{V^2}{L_1} \sin(\eta), \quad (2)$$

where  $V = \|\vec{V}\|$  and  $L_1 = \|\vec{L}_1\|$ . The curved trajectory from the current position  $\mathbf{p}$  to the reference point  $R$  would follow a curvature  $c = 2 \sin(\eta)/L_1$  (and a curve radius equal to  $\frac{1}{|c|}$ ).

#### B. Domain of Attraction

When the path to be followed is a straight line,  $L_1$  is given by  $L_1 = \sqrt{d^2 + L_0^2}$  (see Fig. 1). In the case of a curved path (see Fig. 2), we distinguish between the arc joining  $Q$  to  $R$  through the path, with curvature radius  $R_0$  and arc-length  $2\gamma R_0$ , from the vector  $\vec{L}_0$  also joining  $Q$  to  $R$ . The length of this vector satisfies  $L_0 = 2R_0 \sin \gamma$  and  $L_1$  is given by

$$\begin{aligned} L_1 &= \sqrt{(d \cos(\gamma))^2 + (L_0 + d \sin(\gamma))^2} \\ &= \sqrt{d^2 + L_0^2 \left(1 + \frac{d}{R_0}\right)}. \end{aligned} \quad (3)$$

For a straight path, since  $R_0 = \infty$  ( $\gamma = 0$ ), this simplifies to  $L_1 = \sqrt{d^2 + L_0^2}$ .

The L0 guidance offers advantages over the L1 guidance control, since it enlarges the controller domain of attraction. When applying the L1 guidance control, we must have a backup control strategy for when the vehicle distances more than a fixed  $L_1$  from the path. Therefore, while the domain of attraction of the L1 controller is

$$\{(d, \eta) : d \leq L_1, \eta \in (-\pi/2, \pi/2)\}$$

the domain of attraction of the L0 controller is, as we shall see, the set

$$\{(d, \eta) : d \in \mathbb{R}, \eta \in (-\pi, \pi)\}.$$

Regarding the controller domain of attraction with saturation, we must define three different sets:  $S_1$  that consists of the non-saturated region and  $S_2$  and  $S_3$  which correspond to saturated regions (in which the lateral acceleration computed using Equation 2 does not comply with the maximum allowable trajectory curvature).

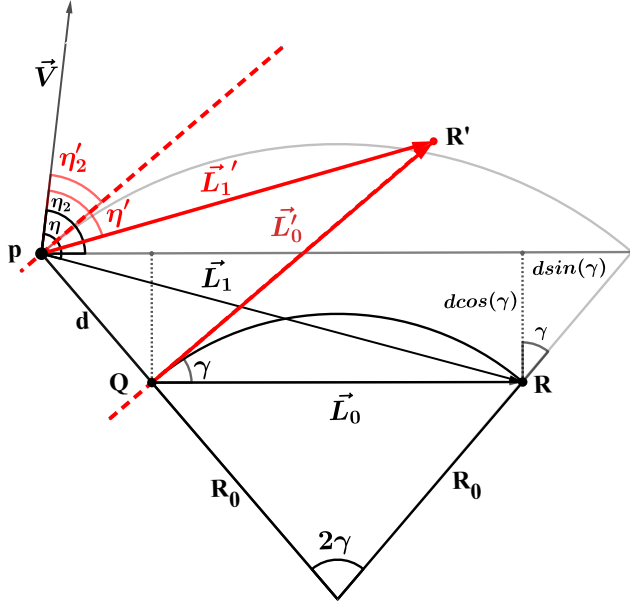


Fig. 2. Variables used in the curved path stability proof.

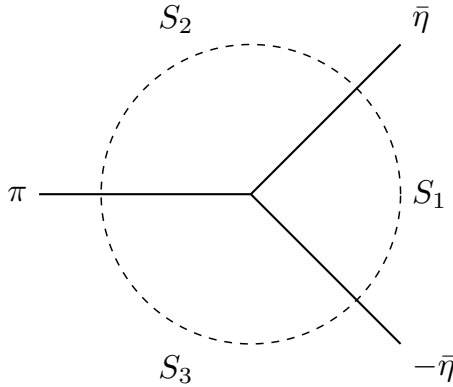


Fig. 3. Saturated and non-saturated state space regions [6].

The first region can then be defined as the set:

$$S_1 := \{(d, \eta) : d \in \mathbb{R}, \eta \in [-\bar{\eta}, \bar{\eta}]\}.$$

where  $\bar{\eta}$  is the angle in  $(0, \pi/2)$  correspondent to the limitations of the vehicle manoeuvrability, which can be related to the minimum curvature radius permitted by the vehicle  $R_{min}$ .

Let  $S_2$  and  $S_3$  be the sets

$$S_2 := \{(d, \eta) : d \in \mathbb{R}, \eta \in (\bar{\eta}, \pi]\},$$

$$S_3 := \{(d, \eta) : d \in \mathbb{R}, \eta \in (-\pi, -\bar{\eta}]\},$$

The sets  $S_1$ ,  $S_2$  and  $S_3$  define three partitions of the global domain of attraction  $S := \{(d, \eta) : d \in \mathbb{R}, \eta \in (-\pi, \pi]\}$  and are represented in Figure 3.

The final Guidance Logic control law is then represented as:

$$a_s(t) = \begin{cases} \frac{2V^2}{L_1} \sin(\eta) & \text{if } (d, \eta) \in S_1, \\ \frac{2V^2}{L_1} \sin(\bar{\eta}) & \text{if } (d, \eta) \in S_2, \\ -\frac{2V^2}{L_1} \sin(\bar{\eta}) & \text{if } (d, \eta) \in S_3, \end{cases} \quad (4)$$

### C. Parameter Limits

Depending on the vehicle manoeuvrability and its non-holonomic constraints, there is a minimum radius defining its possible curvature, *i.e.* there is a minimum radius  $R_{min}$  for which  $R_{min} \leq L_1/(2 \sin(\eta))$ .

This inequality allows us to find a relation between our  $\bar{\eta}$  and the other parameters of the controller.

$$\begin{aligned} R_{min} &\leq \frac{L_1}{2 \sin(|\eta|)} \Leftrightarrow \\ |\eta| &\leq \arcsin\left(\frac{L_1}{2R_{min}}\right) \Leftrightarrow \\ |\eta| &\leq \arcsin\left(\frac{\sqrt{d^2 + (1 + \frac{d}{R_0})L_0^2}}{2R_{min}}\right) = \bar{\eta} \end{aligned}$$

In the case of a straight path, since  $R_0 = \infty$  ( $\gamma = 0$ ), this amounts to:

$$|\eta| \leq \arcsin\left(\frac{\sqrt{d^2 + L_0^2}}{2R_{min}}\right) = \bar{\eta}$$

It is also advisable to choose a  $L_0 < 2R_0$ , since a parameter  $L_0 \geq 2R_0$  may not encounter a reference point  $R$  for small enough cross-track errors  $d$  in a circular path.

## IV. STABILITY ANALYSIS

In this section we prove the stability of the L0 Guidance Logic. We prove that the controller defined in Equation 4 will steer the pair of variables  $(d, \eta)$  in the case of a straight path and  $(d, \eta')$  in the case of a curved path to  $(0, 0)$ .

In order to do this, we will use a set of auxiliary variables, namely a variable  $\eta'_2$  ( $\eta_2$  in a straight path) that will replace  $\eta'$  (or  $\eta$ ) in the equations of motion, however we can observe from Figure 2 (or Figure 4) that when both  $d$  and  $\eta'_2$  are equal to zero so is  $\eta'$ .

These variables and their relations will be explained as needed throughout the proof of stability.

### A. Main Result

The main result in this paper applies to systems with the following dynamics with respect to the path:

$$\begin{cases} \dot{d} &= V \sin(\eta'_2) \\ \dot{\eta}'_2 &= -a_s/V. \end{cases} \quad (5)$$

Here  $d$  is, as before, the cross-track error and  $\eta'_2$  is the angle between the velocity vector and vector  $\vec{L}'_1$ . These variables, which are shown in Figure 2, and its respective equations of motion will be further explained below.

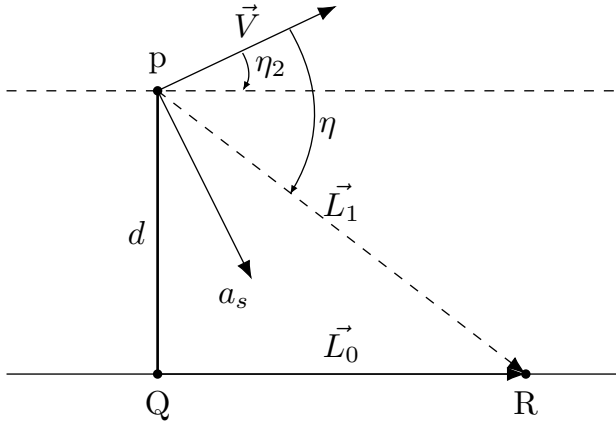


Fig. 4. Variables used in the straight path stability proof [6].

The stability result is established under the following hypotheses

*Hypothesis 1:*  $V \neq 0$ .

*Hypothesis 2:*  $\bar{\eta} < \pi/2$ .

*Hypothesis 3:*  $0 < L_0 < 2R_0$ .

*Remark 1:* Although Hypothesis 1 states that  $V \neq 0$ , throughout the proof it will be assumed, without loss of generality, that  $V > 0$ . Hypothesis 2 is required to guarantee a region in which the Lyapunov function is strictly decreasing. Hypothesis 3 is required in order to guarantee that a reference point  $R$  can be found.

The main result of this work is the following:

*Theorem 1:* Assuming that Hypothesis 1-3 hold, the control law in Equation (4) Asymptotically Stabilizes the dynamical system (5), ensuring convergence to the path.

To show this result, we firstly recall the proof of stability for a straight path shown in [6] and then demonstrate the proof of stability for a curved path.

Both stability proofs will follow three main steps:

- 1) States in the saturated regions ( $S_1$  and  $S_2$ ) will lead to  $S_1$ ;
- 2) The unsaturated set  $S_1$  is invariant;
- 3) We can find a Lyapunov function within  $S_1$  that establishes convergence of the state pair to the origin (Asymptotic Stability).

### B. Straight Path

In this subsection we show that a vehicle using the guidance logic in Equation (4) performs a convergent trajectory to a straight path. In other words, we demonstrate

that the coordinates  $(d, \eta)$  converge to the origin  $(0, 0)$  (or equivalently  $(d, \eta_2)$ , since when  $d = 0$  and  $\eta_2 = 0$ ,  $\eta = 0$  as well).

Consider the following equations of motion

$$\begin{cases} \dot{d} &= V \sin(\eta_2) \\ \dot{\eta}_2 &= -a_s/V, \end{cases} \quad (6)$$

where  $d$ , as mentioned above, is the distance between the vehicle current position and the path and  $\eta_2$  is the angle between the velocity vector ( $\vec{V}$ ) and vector  $\vec{L}_0$ .

$L_1$  represents the magnitude of the vector  $\vec{L}_1$ , which is equal to  $\sqrt{d^2 + L_0^2}$  in the case of a straight path. Figure 4 depicts these variables. We consider the lateral acceleration shown in Equation (4).

1) *States in the Saturated Regions:* We begin by showing that when the system state is in either one of the saturated regions ( $S_2$  and  $S_3$ ) the guidance control will lead the state to  $S_1$ .

We start by showing that when the state  $(d, \eta) \in S_2$ , then the state is driven to  $S_1$ . Considering an angle  $\eta_1$  defined by  $\eta_1 = \eta - \eta_2$ , we have that:

$$\dot{\eta} = \dot{\eta}_1 + \dot{\eta}_2,$$

and from  $\sin(\eta_1) = d/L_1$  we deduce that

$$\dot{\eta}_1 \simeq \frac{\dot{d}}{L_1} = \frac{V}{L_1} \sin(\eta_2).$$

On the other hand and from the dynamics in Equation (6) we find that

$$\dot{\eta}_2 = \frac{-\bar{a}_s}{L_1} = -\frac{2V}{L_1} \sin(\bar{\eta}). \quad (7)$$

From the combination of these two equalities, we obtain

$$\dot{\eta} = \frac{V}{L_1} (\sin(\eta_2) - 2\sin(\bar{\eta})). \quad (8)$$

By Equation 7, in region  $S_2$ , the  $\dot{\eta}_2 < 0$ , therefore, even when  $\sin(\eta_2) - 2\sin(\bar{\eta}) \geq 0$  (which, from Equation 8, would configure an increasing  $\dot{\eta}$ ), this inequality will eventually reduce to a value smaller than zero. Therefore, once  $\dot{\eta} < 0$ ,  $\eta$  will decrease uniformly until the state enters  $S_1$  (*i.e.*  $\eta \leq \bar{\eta}$ ).

An equivalent proof is possible for the case of  $S_3$ , in which it is proven that  $\dot{\eta} > 0$  and therefore  $\eta$  increases until  $\eta \geq \bar{\eta}$ , thus entering in the set  $S_1$ .

2)  *$S_1$  is invariant:* The second part of the proof relates to the invariance of the set  $S_1$ , *i.e.* when the system is in the non-saturated set  $S_1$  it will remain in this set.

We can show invariance of the set by demonstrating that  $\dot{\eta}$  in the boundary of the set points inwards (see [9, Thm 4.2.4.]).

Let us then consider that  $\eta = \pm\bar{\eta}$ . From Equation (8) we have that:

$$\dot{\eta} = \frac{V}{L_1} (\sin(\eta_2) - 2\sin(\bar{\eta})) \text{sign}(\eta). \quad (9)$$

Since  $\bar{\eta} = |\eta| > \eta_2$  we deduce that

$$\eta\dot{\eta} < 0,$$

proving that the velocity in the boundary of  $S_1$  points inwards and therefore  $S_1$  is invariant.

3)  $S_1$  is *Asymptotically Stable*: The final step comprises a Lyapunov Stability Analysis within the unsaturated set  $S_1$ .

Following [6], we consider the Lyapunov function pair based on the kinetic energy and the work associated to the acceleration  $a_s$  in the orthogonal direction to the path:

$$\begin{aligned} \frac{1}{2}m(\dot{d})^2 + \int_0^d ma_s \cos(\eta_2) dy &= \frac{1}{2}m(V \sin(\eta_2))^2 + \\ &+ \int_0^d \frac{2mV^2}{L_1} (\sin(\eta - \eta_2) + \cos(\eta) \sin(\eta_2)) dy. \end{aligned} \quad (10)$$

Omitting the mass  $m$  as well as the last component of the integrand, we find our Lyapunov function candidate:

$$\mathcal{V} = \frac{1}{2} (V \sin(\eta_2))^2 + \int_0^d \frac{2V^2}{\sqrt{L_0^2 + y^2}} \sin(\eta - \eta_2) dy. \quad (12)$$

Owing to the fact that

$$\sin(\eta - \eta_2) = \sin(\eta_1) = \frac{y}{L_1} = \frac{y}{\sqrt{L_0^2 + y^2}}, \quad (13)$$

we can simplify our Lyapunov function to:

$$\begin{aligned} \mathcal{V} &= \frac{1}{2} (V \sin(\eta_2))^2 + V^2 \int_0^d \frac{2y}{L^2 + y^2} dy \\ &= \frac{1}{2} (V \sin(\eta_2))^2 + V^2 (\ln(L_0^2 + d^2) - \ln(L_0^2)) \\ &= \frac{1}{2} (V \sin(\eta_2))^2 + V^2 (\ln(L_1^2) - \ln(L_0^2)). \end{aligned} \quad (14)$$

This equation can be easily shown to be positive definite.

Next, we compute the time derivative of the Lyapunov function along the system trajectory

$$\begin{aligned} \dot{\mathcal{V}} &= \frac{1}{2} V^2 2 \sin(\eta_2) \cos(\eta_2) \dot{\eta}_2 + V^2 \frac{2d}{L^2 + d^2} \dot{d} \\ &= -\frac{2V^3}{L_1} \sin(\eta_2) \left( \cos(\eta_2) \sin(\eta) - \frac{d}{L_1} \right). \end{aligned} \quad (15)$$

Using the relation of Equation (13), we can write Equation (15) as

$$\dot{\mathcal{V}} = -\frac{2V^3}{L_1} \sin(\eta_2) (\cos(\eta_2) \sin(\eta) - \sin(\eta - \eta_2)).$$

Considering the trigonometric functions properties that state that  $\sin(\eta - \eta_2) = \sin(\eta) \cos(\eta_2) - \cos(\eta) \sin(\eta_2)$ , this simplifies to

$$\dot{\mathcal{V}} = -\frac{2V^3}{L_1} \sin^2(\eta_2) \cos(\eta), \quad (16)$$

which, since

$$|\eta| \leq |\bar{\eta}| < \frac{\pi}{2},$$

is a negative semi-definite function.

We can apply the invariant set theorem, as in [10, Them. 3.4], to prove the Asymptotic Stability of this controller.

Given that  $|\eta| < \pi/2$  and  $V > 0$ , the set  $\mathcal{S} := \{(d, \eta_2) : \dot{\mathcal{V}} = 0\}$  must be defined by  $\eta_2 = 0$ . Besides, since in any point where  $d \neq 0$ , the acceleration  $a_s \neq 0$ , which would alter  $\eta_2$ , the largest invariant set within  $\mathcal{S}$  is the origin  $(d, \eta_2) = (0, 0)$ .

Therefore, according to [10, Them. 3.4], we come to the conclusion that the origin  $(d, \eta_2) = (0, 0)$  is Asymptotically Stable.

### C. Curved Path

Parting from the proof of stability of the L0 guidance control for a straight path, we can develop a similar proof for curved paths. However, we must begin by introducing a new set of variables that correspond to a straight path tangent to the curved one at point  $Q$ . This tangent straight path and its variables are shown in Figure 2 highlighted in red.

We introduce a point  $R'$ , distancing  $L_0$  from  $Q$  in the tangent straight path represented as a dashed red line. The vector  $\vec{L}'_1$  (with magnitude  $L'_1$ ) joins the current vehicle position  $\mathbf{p}$  and the point  $R'$ . The angles  $\eta'_1$  and  $\eta'_2$  are the angles between the vehicle velocity vector  $\vec{V}$  and the vector  $\vec{L}'_1$  and the vector  $\vec{L}'_0$ , respectively. For the stability proof we also need to introduce an angle  $\eta'_1$  which is defined similarly to  $\eta_1$  as  $\eta'_1 = \eta' - \eta'_2$ .

In this case we define our state variables as  $(d, \eta'_2)$  which we would like to reach the origin, representing that the vehicle is on the path. This is equivalent to a system using states  $(d, \eta')$ , since when  $d = 0$  and  $\eta'_2 = 0$ , then  $\eta' = 0$  (and  $\eta = \gamma$ ). The equations of motion for the system are represented in Equation (5).

When on the path, since  $d = 0$  and  $\eta = \gamma$ , the centripetal acceleration will be equal to  $a_s = \frac{2V^2 \sin(\eta)}{L_1} = \frac{2V^2 \sin(\gamma)}{L_0} = \frac{V^2}{R_0}$ , which is the required acceleration for the vehicle to remain on the curved path with radius  $R_0$ .

1) *States in the Saturated Regions*: As in the proof for a straight path, we begin by demonstrating that when  $(d, \eta) \in S_2$ , the state is led to  $S_1$ .

We have that  $\eta = \eta' + \gamma$  and that

$$\dot{\eta} = \dot{\eta}' = \dot{\eta}'_1 + \dot{\eta}'_2.$$

From this point on, the proof is in every step similar to the one of the straight path, being  $\sin(\eta'_1) = d/L'_1$  from which we deduce that

$$\dot{\eta}'_1 \simeq \frac{\dot{d}}{L'_1} = \frac{V}{L'_1} \sin(\eta'_2).$$

From the equations of motion shown in Equation (5), we have

$$\dot{\eta}'_2 = \frac{-\bar{a}_s}{L_1} = -\frac{2V}{L_1} \sin(\bar{\eta}). \quad (17)$$

Finally, combining these equalities

$$\dot{\eta} = \frac{V}{L_1} (\sin(\eta'_2) - 2 \sin(\bar{\eta})).$$

Similarly to the case of the straight path, we see that when  $\sin(\eta'_2) - 2\sin(\bar{\eta}) \geq 0$  and due to Equation (17),  $\eta'_2$  decreases until  $\sin(\eta'_2) - 2\sin(\bar{\eta}) < 0$ . Therefore, we conclude that  $\eta$  decreases uniformly until  $\eta \leq \bar{\eta}$  and  $(d, \eta) \in S_1$ , since  $\dot{\eta} = \eta' < 0$ .

2)  $S_1$  is invariant: The second step consists on proving the invariance of  $S_1$ . Considering, once again, the case when the state is on the boundary of the unsaturated set, thus  $\eta = \pm\bar{\eta}$ , we have that

$$\dot{\eta} = \frac{V}{L_1}(\sin(\eta'_2) - 2\sin(\bar{\eta}))\text{sign}(\eta).$$

Since  $\bar{\eta} = |\eta| > \eta'_2$  we deduce

$$\eta\dot{\eta} < 0.$$

Consequently, the velocity in every point in the boundary of  $S_1$  is pointing inwards, not permitting the system to leave the unsaturated set (see [9, Thm. 4.2.4]).

3)  $S_1$  is Lyapunov Asymptotically Stable: In order to prove Asymptotical Stability we will use a similar Lyapunov Function pair as in Equation (14) from the straight path case:

$$\begin{aligned} \mathcal{V} &= \frac{1}{2}(V \sin(\eta'_2))^2 + V^2(\ln(L_1^2) - \ln(L_0^2)) \\ &= \frac{1}{2}(V \sin(\eta'_2))^2 \\ &\quad + V^2\left(\ln\left(d^2 + L_0^2\left(1 + \frac{d}{R_0}\right)\right) - \ln(L_0^2)\right). \end{aligned} \quad (18)$$

This function is positive definite with respect to both state variables. Its derivative along the trajectory is then

$$\begin{aligned} \dot{\mathcal{V}} &= \frac{1}{2}V^2 2\sin(\eta'_2)\cos(\eta'_2)\eta'_2 + 2V^2\frac{d + 2L_0\sin(\gamma)}{L_1^2}\dot{d} \\ &= -\frac{2V^3}{L_1}\sin(\eta'_2)\left(\cos(\eta'_2)\sin(\eta) - \frac{d + 2L_0\sin(\gamma)}{L_1}\right). \end{aligned} \quad (20)$$

This can be shown to be equal to

$$\dot{\mathcal{V}} = -\frac{2V^3}{L_1}\sin(\eta'_2)(\cos(\eta'_2)\sin(\eta) - \sin(\eta_1 + \gamma)). \quad (21)$$

Since  $\gamma = \eta_2 - \eta'_2$ , we have that

$$\dot{\mathcal{V}} = -\frac{2V^3}{L_1}\sin(\eta'_2)(\cos(\eta'_2)\sin(\eta) - \sin(\eta - \eta'_2)), \quad (22)$$

which in combination with the fact that  $\sin(\eta - \eta'_2) = \sin(\eta)\cos(\eta'_2) - \cos(\eta)\sin(\eta'_2)$  culminates in our Lyapunov function time-derivative:

$$\dot{\mathcal{V}} = -\frac{2V^3}{L_1}\sin(\eta'_2)^2\cos(\eta), \quad (23)$$

which is a negative semi-definite function for  $|\eta| \leq \frac{\pi}{2}$ .

Considering the set  $\mathcal{S} := \{(d, \eta'_2) : \dot{\mathcal{V}} = 0\}$ , since  $V > 0$  and  $|\eta| < \frac{\pi}{2}$ , we must have  $\eta'_2 = 0$ . Besides,  $\{(d, \eta'_2) =$

$(0, 0)\}$  is the largest invariant set in  $\mathcal{S}$ , due to the fact that in any other case (*i.e.*  $d \neq 0$ ) the acceleration conveyed by the guidance law will be  $a_s \neq 0$  steering the system out of  $\mathcal{S}$ .

Therefore, applying the invariant set theorem found in [10, Thm. 3.4], we can conclude Asymptotical Stability of the L0 guidance control for curved paths.

## V. CONCLUSIONS

We have studied a path-following guidance method called L0 Guidance and have analysed its stability properties. It is shown that a nonholonomic system, that might have a minimum turning radius, can be made to converge to either a straight or a curved path when using L0 Guidance. This convergence can be guaranteed even when the vehicle is far from the path, significantly enlarging the domain of attraction when compared to the well-known L1 guidance, since in the former method the stability guarantees are not limited to the case when the cross-track error is smaller than the fixed tuning parameter.

## REFERENCES

- [1] A. P. Aguiar, J. P. Hespanha, and P. V. Kokotović, "Performance limitations in reference tracking and path following for nonlinear systems," *Automatica*, vol. 44, no. 3, pp. 598–610, 2008.
- [2] T. I. Fossen, "An adaptive line-of-sight (ALOS) guidance law for path following of aircraft and marine craft," *IEEE Transactions on Control Systems Technology*, 2023.
- [3] N. Hung, F. Rego, J. Quintas, J. Cruz, M. Jacinto, D. Souto, A. Potes, L. Sebastiao, and A. Pascoal, "A review of path following control strategies for autonomous robotic vehicles: Theory, simulations, and experiments," *Journal of Field Robotics*, vol. 40, no. 3, pp. 747–779, 2023.
- [4] S. Park, J. Deyst, and J. How, "A New Nonlinear Guidance Logic for Trajectory Tracking," in *AIAA Guidance, Navigation, and Control Conference and Exhibit*, American Institute of Aeronautics and Astronautics, 2004.
- [5] S. Park, J. Deyst, and J. How, "Performance and Lyapunov Stability of a Nonlinear Path Following Guidance Method," *Journal of Guidance, Control and Dynamics*, vol. 30, no. 6, 2007.
- [6] G. B. Silva, L. T. Paiva, and F. A. Fontes, "A path-following guidance method for airborne wind energy systems with large domain of attraction," in *2019 American Control Conference (ACC)*, pp. 2771–2776, IEEE, 2019.
- [7] M. C. Fernandes, L. T. Paiva, and F. A. Fontes, "A Model Predictive Control Scheme to Improve Performance of a Path-Following Controller for Airborne Wind Energy," (Berlin), July 2020.
- [8] M. C. R. M. Fernandes, S. Vinha, L. T. Paiva, and F. A. C. C. Fontes, "L0 and l1 guidance and path-following control for airborne wind energy systems," *Energies*, vol. 15, no. 4, 2022.
- [9] F. H. Clarke, Y. S. Ledyaev, R. J. Stern, and P. R. Wolenski, *Nonsmooth analysis and control theory*, vol. 178. Springer Science & Business Media, 2008.
- [10] J.-J. E. Slotine, W. Li, and others, *Applied nonlinear control*, vol. 199. Prentice hall Englewood Cliffs, NJ, 1991.